^{18}F-FDG PET/CT for the Prediction and Detection of Local Recurrence After Radiofrequency Ablation of Malignant Lung Lesions

Amit Singnurkar[1], Stephen B. Solomon[2], Mithat Gönen[3], Steven M. Larson[1], and Heiko Schöder[1]

[1]Department of Radiology/Nuclear Medicine Service, Memorial Sloan-Kettering Cancer Center, New York, New York; [2]Department of Radiology/Interventional Radiology Service, Memorial Sloan-Kettering Cancer Center, New York, New York; and [3]Department of Epidemiology and Biostatistics, Memorial Sloan-Kettering Cancer Center, New York, New York

The utility of ^{18}F-FDG PET/CT for response assessment in malignant lung tumors treated with radiofrequency ablation (RFA) and for the detection and prediction of local recurrence was investigated. **Methods:** Between December 17, 2003, and April 9, 2008, 68 consecutive patients (mean age, 68 y) with 94 pulmonary lesions, including metastases (n = 38) and primary lung cancers (n = 44), underwent RFA. Because of inadequate imaging follow-up in 12 patients, only 82 lesions were analyzed (CT scans, n = 82; ^{18}F-FDG PET/CT scans, n = 62). The median follow-up was 25 mo (range, 12–66 mo). A baseline study was defined as ^{18}F-FDG PET/CT performed no more than 3 mo before RFA. The first postablation scan was defined as PET/CT performed between 1 and 4 mo after RFA; additional follow-up studies were obtained in some cases between 6 and 12 mo after RFA. The unidimensional maximum diameter of the lesion was recorded on a pretherapy diagnostic CT scan or on the CT component of a pretherapy ^{18}F-FDG PET/CT scan, whichever was obtained most recently, using lung windows. Maximum standardized uptake values (SUVs) were recorded for all lesions imaged by ^{18}F-FDG PET/CT. ^{18}F-FDG uptake patterns on post-RFA scans were classified as favorable or unfavorable. Survival and recurrence probabilities were estimated using the Kaplan–Meier method. Uni- and multivariate analyses were also performed. **Results:** Before RFA, factors predicting greater local recurrence-free survival included initial lesion size less than 3 cm (P = 0.01) and SUV less than 8 (P = 0.02), although the latter was not an independent predictor in multivariate analysis. Treated metastases recurred less often than treated primary lung cancers (P = 0.03). Important post-RFA factors that related to reduced recurrence-free survival included an unfavorable uptake pattern ($P < 0.01$), post-RFA SUV ($P < 0.01$), and an increase in SUV over time after ablation (P = 0.05). **Conclusion:** ^{18}F-FDG PET/CT parameters on both preablation and postablation scans may predict local recurrence in patients treated with RFA for lung metastases and primary lung cancers.

Key Words: radiofrequency ablation; ^{18}F-FDG PET/CT; treatment response; lung cancer

J Nucl Med 2010; 51:1833–1840
DOI: 10.2967/jnumed.110.076778

Primary lung cancer is one of the most common malignancies in the United States, with an estimated 215,020 new cases, comprising approximately 15% of new cancer diagnoses, and 161,840 deaths accounting for close to 29% of cancer deaths in 2008 (*1*). The lungs are also a frequent site for metastases from extrapulmonary neoplasms such as breast, colorectal, prostate, head and neck, and renal cancers. Treatment options for lung cancer and lung metastases include surgical resection, external-beam radiotherapy, chemotherapy, targeted therapies (such as tyrosine kinase inhibitors), and thermal ablation procedures, such as radiofrequency ablation (RFA). RFA of lung lesions has gained increasing acceptance as a viable alternative for the treatment of pulmonary malignancies (*2–4*). RFA is increasingly used in patients who are unable to undergo surgery or for palliation of patients' symptoms. The technique entails the insertion of an ablation needle into the lesion and the generation of localized thermal energy via an alternating current, supplied by a radiofrequency generator. The resulting ionic agitation in the tissue generates temperatures upward of 90°C and leads to thermal coagulative necrosis of the lesion and surrounding normal pulmonary parenchyma forming the ablation margin (*5*). In experienced hands, RFA is a relatively safe procedure, with low morbidity and mortality; pneumothorax is the most frequent procedure-related complication (*6*). Although the immediate effectiveness of RFA and short-term recurrence rates are well documented (*3,7,8*), there is a paucity of information regarding the long-term effectiveness of this procedure as compared with established treatment modalities including external-beam radiotherapy and surgical resection.

^{18}F-FDG PET/CT is now a standard diagnostic imaging test for the staging and follow-up of lung cancer and assess-

Received Mar. 3, 2010; revision accepted May 19, 2010.
For correspondence or reprints contact: Amit Singnurkar, Department of Nuclear Medicine, Henderson General Hospital, 711 Concession St., Hamilton, Ontario, Canada L8V 1C3.
E-mail: amitsingnurkar@gmail.com

ment of lung nodules (*9–15*). In addition, this imaging modality is increasingly used for response assessment in lung cancer. Several reports have documented changes in ^{18}F-FDG uptake pattern in response to external-beam radiotherapy (*16,17*), chemotherapy (*18*), or biologic agents (*19*). Building on these reports, it was the aim of the current study to investigate the utility of ^{18}F-FDG PET/CT for response assessment in RFA-treated lung lesions and for the detection and prediction of local recurrence. We define PET patterns, which (in conjunction with clinical parameters) influence the probability for local recurrence and might prove useful in the future when selecting patients likely to be cured by RFA, and patients at higher risk for local recurrence who may benefit from closer surveillance.

MATERIALS AND METHODS

In this retrospective study, we evaluated 68 consecutive patients who underwent RFA for both primary and metastatic lung lesions between December 2003 and April 2008 and in whom ^{18}F-FDG PET/CT was performed at baseline before therapy or during follow-up. Data collection and analysis in this study (compliant with the Health Insurance Portability and Accountability Act) were approved by the institutional review board; patient informed consent was not required. All patients had biopsy-proven non–small cell lung cancer or biopsy-proven extrapulmonary cancers (patients with lung metastases) and at least 12 mo of follow-up. All primary lung cancers were characterized histopathologically by institutional staff pathologists. Growing pulmonary metastases were assumed to be related to the known, biopsy-proven primary cancer located elsewhere.

Ambiguous lung lesions, in cases with more than 1 primary tumor ($n = 1$), were biopsied. Patients with inadequate follow-up and lack of metabolic imaging at the time intervals defined in the "Imaging" section were excluded from the analysis.

Radiofrequency Ablation

For 55 lesions, RFA was performed with the Cool-Tip RFA device (Covidien), which consists of a radiofrequency generator and single- or parallel-needle electrodes. Nine lesions were ablated with the LeVeen Needle Electrode and RF3000 radiofrequency generator (Boston Scientific) and 18 lesions with the RITA Starburst XL Electrosurgical Device and RITA 1500 generator (AngioDynamics, Inc.). The operator chose the device, using the expected shape and size of the ablation. Ablation was performed with anesthesia, as per the manufacturer's protocols, with CT guidance.

Imaging

A baseline study (pretherapy scan) was defined as ^{18}F-FDG PET/CT performed no more than 3 mo before RFA. The unidimensional maximum diameter of the lesion was recorded on a pretherapy diagnostic CT scan or the CT component of a pretherapy ^{18}F-FDG PET/CT scan, whichever was done most recently, using lung windows. If an ^{18}F-FDG PET/CT scan was available, the baseline standardized uptake value (SUV) of the pulmonary lesion was recorded. After RFA, imaging studies were ordered by the treating interventional radiologists as considered clinically appropriate. In general, either a chest CT scan or an ^{18}F-FDG PET/CT scan was ordered 1–4 mo after the ablation, and subsequent imaging follow-up was based on these initial results and patient symptoms.

The first postablation scan was defined as PET/CT done between 1 and 4 mo after RFA; additional follow-up studies were obtained in some cases between 6 and 12 mo after RFA. Because of the retrospective nature of the study, patients had ^{18}F-FDG PET/CT studies available only in certain time intervals. For example, some patients had a postablation PET/CT scan and additional subsequent PET/CT scans but no pretherapy scan, some patients had only pretherapy scans, and some had both. In addition, the time point for posttherapy scans varied.

For PET/CT, patients fasted for at least 6 h before injection of 444–555 MBq of ^{18}F-FDG, but liberal water was allowed. On arrival in the nuclear medicine clinic, plasma glucose was checked before ^{18}F-FDG injection and was less than 200 mg/dL in all patients. ^{18}F-FDG was then injected intravenously, and image acquisition was started 60–90 min afterward. During the uptake period, patients rested quietly in the injection room. All PET/CT studies were acquired on combined PET/CT tomographs, either Biograph (Siemens Medical Solutions, Inc.) (*20*), Discovery LS (GE Healthcare) (*21*), Discovery ST (GE Healthcare) (*22*), or Discovery STE (GE Healthcare) (*23*). After the topogram (scout view), a low-dose CT scan was obtained from the skull base to the inguinal region. For the Biograph device, a spiral CT scan was acquired using the following parameters: 50 effective milliamperes; 130 kVp; scan width, 5 mm; collimation, 4 mm; and feed or rotation, 12 mm. For patients with a body mass of more than 90 kg, effective mAs were increased to 85. For the Discovery devices, a spiral CT scan was acquired in 0.8 s/rotation using 80 mA; 140 kVp; slice thickness, 5 mm; and interval, 4.25 mm in high-sensitivity mode. Immediately on completion of the CT scan, the PET scan was acquired for 3–5 min per bed position, with a 5-slice (2.1-cm) overlap between bed positions for the Discovery and a 13-slice (3.2-cm) overlap for the Biograph. The CT data were used for attenuation correction.

Pre- and posttreatment CT scans of the chest were obtained without intravenous contrast on 16- or 64-detector-row scanners (LightSpeed; GE Healthcare), with the field of view extending from the supraclavicular region to the adrenal glands, using the following parameters: 120 kV; 150 mA (adjusted for large patients); pitch, 0.984; scan rotation speed, 39.37 mm/s; slice thickness/spacing, 5 × 5 mm; and tube rotation speed, 0.5-s rotation. Images were obtained with the patient supine and in deep-inspiration breath-hold and reconstructed using a high-spatial-frequency (lung) algorithm.

PET/CT Image Interpretation

For this study, all PET/CT studies were reviewed retrospectively by 2 nuclear medicine physicians. In all cases, attenuation-corrected images were reviewed on a picture-archiving and communication system workstation (AW suite; GE Healthcare), displaying a maximum-intensity-projection image and at least transaxial PET, CT, and PET/CT fusion images. Baseline and follow-up image datasets were displayed in parallel. ^{18}F-FDG uptake was considered abnormal when it was focal (rather than diffuse), outside normal anatomic structures (such as blood vessels and muscles) seen on the companion CT scan, and of an intensity greater than background blood-pool activity or uptake in adjacent normal lung. Maximum SUVs, normalized to body weight, were measured with volumetric regions of interest, avoiding areas of higher activity in adjacent tissues such as the hila, mediastinum,

and heart. In all cases, the structural appearance of the lung lesions after ablation and, when available, the SUV in postablation scans were recorded.

On PET/CT studies performed between 1 and 4 mo after ablation, the pattern of ^{18}F-FDG uptake was characterized as diffuse, focal, heterogeneous, rim, and rim plus focal uptake (with focal uptake either corresponding to the site of the original lesion or at a different location; Fig. 1). Diffuse uptake was defined as homogeneous ^{18}F-FDG uptake, with smooth tapering borders enveloping the postablation mass and a portion of the surrounding structurally normal pulmonary parenchyma circumferentially. Focal uptake was characterized by an abrupt drop-off of activity at the boundaries of the active area, involving either the entire postablation mass or a portion of it centrally or peripherally. Heterogeneous uptake was defined as an area of increased ^{18}F-FDG uptake interspersed by areas of lesser uptake. Rim uptake and rim plus focal uptake were defined as ringlike tracer uptake at the periphery of the postablation mass; rim plus focal also had an eccentric focus of uptake fusing to the peripheral uptake ring. We further categorized the postablation ^{18}F-FDG uptake into favorable and unfavorable patterns using post hoc analysis of the outcome data. The favorable ^{18}F-FDG patterns included diffuse uptake, heterogeneous uptake, rim uptake, and rim uptake with additional focal uptake at a site different from the ablated tumor nodule. Unfavorable ^{18}F-FDG uptake included focal uptake and rim uptake with additional focal uptake in a location that corresponded to the original tumor nodule. This categorization is essentially based on our experience that posttreatment inflammation does not generally appear focal but rather as rim or mild heterogeneous uptake; conversely, focal uptake suggests residual pockets of viable tumor that were not ablated sufficiently.

In addition to uptake pattern, the SUV for the ablated lung lesion was recorded. On postablation scans, we also assessed the rim ratio, defined as the ratio of the outer edge of the ^{18}F-FDG rim surrounding an ablated lung lesion to the maximum transverse diameter of the original lesion. Because the rim uptake was not always circular, rim size was calculated by taking the average of the maximum transverse diameter and the perpendicular axis of the postablation margin. On subsequent ^{18}F-FDG PET/CT studies performed between 6 and 12 mo after ablation, only the lesional SUVs were recorded.

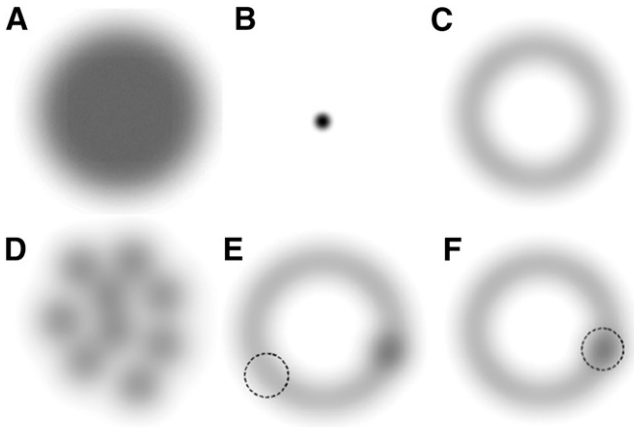

FIGURE 1. Patterns of uptake on post-RFA ^{18}F-FDG PET/CT images: diffuse (A), focal (B), rim (C), heterogeneous (D), rim plus focal with focus not corresponding to site of original lesion (E), and rim plus focal with focus corresponding to site of original lesion (F). Dotted circles represent location of original lesion.

Data Analysis

The primary endpoint of this study was local recurrence at the site of RFA. Recurrence was defined as new nodularity on the CT scan after the first postablation scan, increase in size of the ablated lesion on a subsequent scan, biopsy confirmation, increase in SUV of the ablated lesion by more than 50% between the postablation and subsequent follow-up scans, or new focal ^{18}F-FDG uptake in the ablated lung lesion on follow-up scans. Only 5 lesions were thought to be recurrences based on PET, and 3 lesions were biopsy-confirmed to be recurrences. The remaining lesions were characterized as recurrences using solely CT criteria. The follow-up time was calculated from the date of treatment to the date of the last contact or death. Time to local failure was calculated from the date of treatment completion to the date of a relevant event. Survival and recurrence probabilities were estimated using the Kaplan–Meier method and compared across groups using the log-rank test. Continuous variables such as SUV and size were analyzed using a univariate Cox regression model. The best cutoff points for these variables were located using the maximal χ^2 method (*24*). Multivariate analysis was performed using Cox regression. Because of the limitations of sample size and follow-up, only size and SUV were included in the multivariate analysis.

RESULTS

Between December 17, 2003, and April 9, 2008, 68 consecutive patients (35 women, 33 men; mean age, 68 y; age range, 16–87 y) with 94 lung lesions, including metastases and primary lung cancers, underwent RFA. These patients had received a range of pre-RFA therapies including surgery and radiotherapy, whereas some had received no pre-RFA treatment. Because of inadequate imaging follow-up in 12 patients, only 82 lesions were analyzed. The median follow-up was 25 mo (range, 12–66 mo).

Pretherapy PET/CT scans were available for 40 lesions (Fig. 2). Thirty-one of these 40 lesions were also assessed by at least 1 PET/CT scan during follow-up (13 lesions on PET/CT only within 1–4 mo after therapy, an additional 14 lesions on initial PET/CT within 1–4 mo after therapy and on subsequent later scans, and 4 lesions on PET/CT only beyond 4 mo). For 9 lesions, a CT-alone scan was obtained, and no PET/CT scan was obtained after therapy.

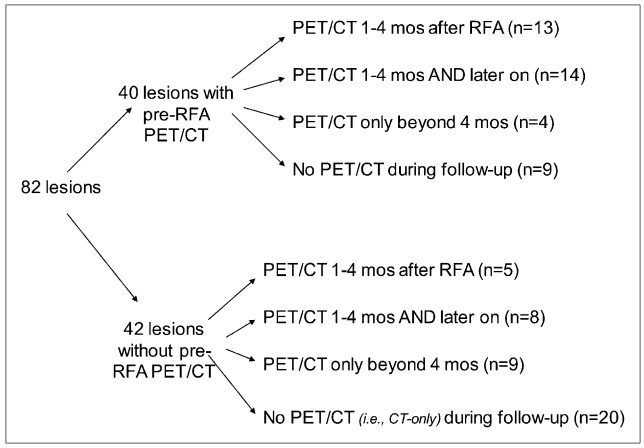

FIGURE 2. Imaging follow-up of ablated lesions.

Forty-two lesions were not assessed by PET/CT before RFA. However, in this cohort, 22 lesions were assessed by at least 1 PET/CT scan after therapy (5 lesions on PET/CT between 1 and 4 mo after RFA, an additional 8 lesions on PET/CT between 1 and 4 mo and at later times, and another 9 lesions on PET/CT only beyond 4 mo after RFA).

Among the 82 lung lesions evaluated, there were 44 primary tumors and 38 metastases (Table 1). The average maximum transverse diameter of these lesions was 2.0 cm (range, 0.7–5.2 cm), and the average maximum preablation SUV was 7.7 (range, 0.6–41.0). Two sarcoma metastases (in 1 patient) had SUVs of 0.6 and 0.8, and both were less than 1.5 cm. All other lesions had an SUV equal to or greater than 1.3.

Preablation Findings

Pathology. Of the 44 primary pulmonary lesions treated mostly with salvage therapy after prior radiation, surgery, or chemotherapy, 20 (45%) recurred locally. The most common histologies treated were adenocarcinoma and squamous cell carcinoma (n = 29), and recurrence was noted in approximately one half (n = 17) of these (Table 1). Among the 38 pulmonary metastases, only 8 (21%) recurred locally; in particular, only 1 of 20 patients with colorectal cancer metastases to the lungs had evidence of local recurrence (Table 1). The recurrence-free survival was better in patients with metastatic lesions than in those with primary lung cancer (P = 0.029). Patients with lung metastases from colorectal cancer had a better recurrence-free survival than patients with other lung metastases or primary lung cancers (1-y recurrence-free survival of 95%, 71%, and 64%, respectively; P = 0.021). The average size of treated colorectal cancer metastases was 1.7 cm, compared with 2.0 cm for the overall average. Nevertheless, the apparent better outcome for colorectal metastases should be interpreted with caution, because there may have been patient referral bias.

Lesion Size. Among the 82 lesions with sufficient follow-up, preablation size correlated with recurrence-free survival (Fig. 3). The mean preablation size of lesions recurring after RFA was 2.4 cm, as compared with 1.8 cm for nonrecurring lesions. A cutoff of 3 cm best dichotomized recurring from nonrecurring lesions, and there was a significant (P = 0.015) decrease in recurrence-free survival in patients with lesions measuring greater than 3 cm (n = 12). The HR for size was 1.93 ($P < 0.01$), suggesting that tumors larger than 3 cm had nearly twice the risk of recurrence of smaller lesions.

SUV. A preablation ^{18}F-FDG PET/CT scan was available for 40 lesions. The mean SUV for tumors recurring locally was 9.8, as compared with 6.7 for nonrecurring lesions. Recurrence-free survival in patients with an SUV greater than 8 (n = 10) was significantly (P = 0.025) shorter when using a best cutoff SUV of 8. The hazard ratio (HR) was 1.04 (P = 0.04). In a multivariate analysis that also included lesion size, however, preablation SUV was not an independent predictor for recurrence-free survival (P = 0.36, HR = 1.02). Conversely, size was independent of SUV as a predictor (P = 0.001, HR = 2.21).

Postablation Findings

For the 40 lesions imaged with PET/CT between 1 and 4 mo after RFA, we analyzed the influence of uptake pattern, SUV, and ablation margins, in the form of rim ratios, on recurrence-free survival. In addition, in a subset of 27 of these 40 lesions, which had also been imaged before RFA, we investigated whether changes in SUV from the preablation scan to the postablation scan were related to the rate of recurrence. Finally, in another subset (22 of the 40 lesions), which had been imaged with ^{18}F-FDG PET/CT initially within 4 mo after RFA and additionally at later times between 6 and 12 mo, we evaluated the effect of subsequent changes in SUV over time.

Uptake Pattern. We dichotomized the postablation ^{18}F-FDG uptake into favorable (n = 28) and unfavorable (n = 12) patterns (Table 2). The favorable ^{18}F-FDG patterns included diffuse uptake, heterogeneous uptake, rim uptake (Fig. 4), and rim uptake with additional focal uptake at a site different from the ablated

TABLE 1
Local Recurrence According to Pathologic Subtype of Pulmonary Lesion

Pathology	*n*	Recurrence	Nonrecurrence
Primary pulmonary lesion	44	20	24
Adenocarcinoma	18	8	10
Squamous cell carcinoma	10	7	3
Undifferentiated non–small cell carcinoma	10	4	6
Adenosquamous carcinoma	1	1	—
Bronchioalveolar carcinoma	3	—	3
Small cell carcinoma	2	—	2
Metastatic lesion	38	8	30
Colorectal	20	1	19
Sarcoma	5	1	4
Fibrosarcoma	1	—	1
Head and neck squamous cell carcinoma	1	—	1
Adrenal	3	1	2
Breast	1	—	1
Esophageal	1	1	—
Insulinoma	1	—	1
Germ cell	1	—	1
Renal	2	2	—
Adenocarcinoma, unknown primary	1	1	—
Carcinoma, unknown primary	1	1	—

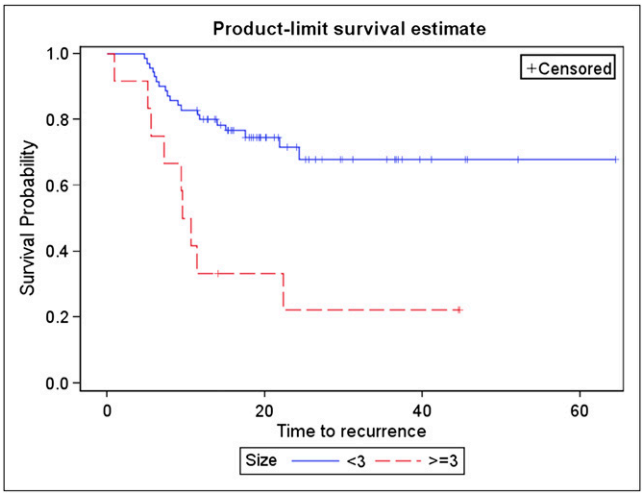

FIGURE 3. Kaplan–Meier curves for recurrence-free survival according to pretreatment lesion size (cm).

tumor nodule. Unfavorable ^{18}F-FDG uptake included focal uptake and rim uptake with additional focal uptake in a location that corresponded to the original tumor nodule (Fig. 5). We observed local recurrences in 9 of 28 patients with favorable uptake pattern, as compared with 10 recurrences in the 12 patients with unfavorable uptake pattern, with a significant decrease in time to recurrence in those lesions with unfavorable uptake ($P = 0.0012$; Fig. 6).

SUV and ΔSUV. SUV measured on the initial postablation scan was a significant predictor of recurrence-free survival ($P = 0.003$, HR = 2.63). Recurring lesions had an average SUV of 9.8 (range, 0.8–38.1; median, 7.8) versus 6.2 (range, 0.6–41.0; median, 4.4) for nonrecurring lesions. In contrast, changes in SUV between pre- and postablation scans varied widely. The mean ΔSUV was −3.2 (range, −18.3 to +7.7) and −5.1 (range, −38.9 to +1.7), respectively, for recurring and nonrecurring lesions. Accordingly, ΔSUV did not predict recurrence-free survival ($P = 0.61$, HR = 1.04).

Rim Ratios. Twenty-one patients with either rim uptake or rim plus focal uptake were evaluated. For lesions that recurred locally, the average rim ratio was 1.8 (range, 0.7–3.0), as compared with 2.8 for nonrecurrences (range, 1.3–4.6). Higher rim ratios showed a trend toward predicting recurrence-free survival ($P = 0.09$, HR = 0.52). In other words, the higher the ratio between the size of the postablation margin and the lesion, the greater the chance for recurrence-free survival.

TABLE 2
Local Recurrence According to Pattern of Uptake on Post-RFA Scan

Pattern	Recurrence	Nonrecurrence
Favorable		
Diffuse	5	10
Heterogeneous	0	1
Rim	3	6
Rim plus focal, corresponding	8	1
Unfavorable		
Focal	2	1
Rim plus focal, not corresponding	1	2

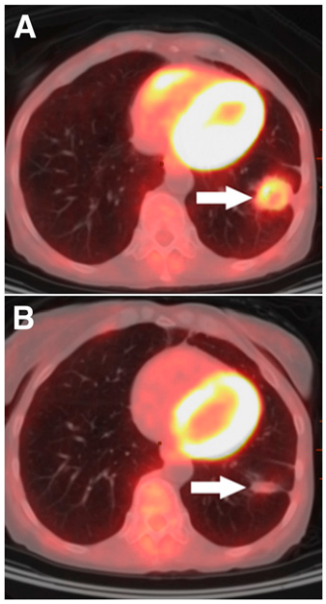

FIGURE 4. Follow-up after RFA for primary non–small cell lung adenocarcinoma. ^{18}F-FDG PET/CT image at 4.5 mo after RFA (A) shows typical early pattern of ring of low-grade (SUV, 3.0) metabolic activity (arrow), and ^{18}F-FDG PET/CT image at 9 mo after RFA (B) shows interval decrease in metabolic activity (arrow) (SUV, 0.8).

DISCUSSION

This study showed that ^{18}F-FDG PET/CT may be a useful tool for assessing treatment response to RFA and predicting the likelihood of local recurrence. We identified pre- and posttherapy imaging features associated with local recurrence. Among pretherapy findings, tumor size was a

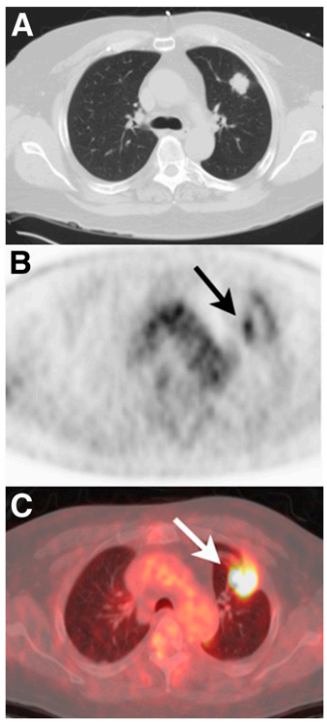

FIGURE 5. Local recurrence with rim plus focal uptake. CT image (A) shows left upper lobe pulmonary metastasis before RFA, and transaxial ^{18}F-FDG PET image at 6 wk after RFA (B) shows rim plus focal uptake with focal uptake corresponding to site of original lesion (arrow). (C) No treatment was performed; PET/CT fusion image obtained 3 mo later shows interval progression (arrow). This lesion was then surgically resected and histopathology proved local recurrence.

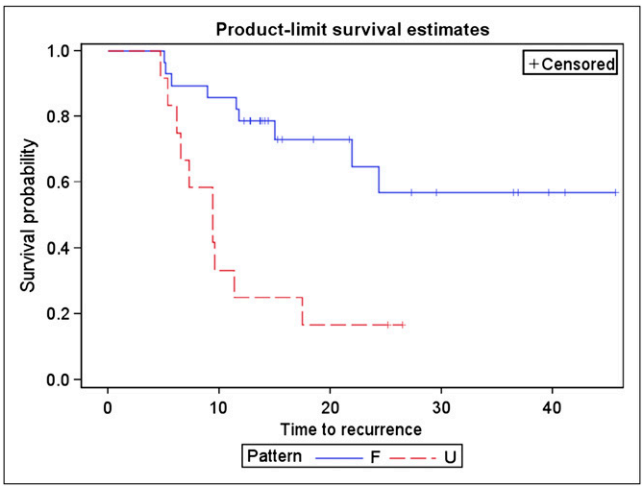

FIGURE 6. Kaplan–Meier curves showing recurrence-free survival according to pattern of ^{18}F-FDG uptake. F = favorable; U = unfavorable.

significant predictor of suboptimal treatment response with RFA. Specifically, patients with tumors greater than 3 cm showed a lower recurrence-free survival, which is concordant with findings in the literature (*8,25,26*). However, this trend may be more a reflection of current technical limitations of RFA, rather than of tumor biology. In addition to size, our univariate analysis also suggested high pretherapy SUV as a predictor of local recurrence, but this predictor was not independent of lesion size in the multivariate analysis. Indeed, because partial-volume effects cause an underestimation of the true activity concentration in smaller lung tumors, lesions with greater size (in particular, when greater than twice the resolution of the PET camera) tend to have higher SUVs (*27*). In addition, for technical reasons successful RFA is more difficult to achieve in larger lesions. Finally, similar to observations in prior studies (*28,29*), we noticed that ablated metastases recurred less frequently than did primary lung cancers. However, most of the primary lung cancer ablations were done as salvage procedures after prior radiation, chemotherapy, or surgery, making them more challenging than the de novo metastasis. In our study, colorectal cancer metastases were more responsive to thermal ablation than other tumors. Although their average size was slightly smaller than the other lesions (1.7 vs. 2.0 cm), it is unlikely that this alone explains differences in outcome. This question deserves further study in the future.

On postablation scans, we defined 6 patterns of ^{18}F-FDG uptake: diffuse, focal, heterogeneous, rim, and rim plus focal, with focal uptake either at a site of original disease or at another site. Rim uptake was previously shown as a favorable indicator of normal postablation inflammation around the treated tumor (*30*). Other favorable uptake patterns included diffuse, heterogeneous, and rim plus focal uptake when the focal uptake did not correspond to the original tumor nodule. The combination of rim plus focal uptake deserves further comment: on the basis of our findings, a rim of ^{18}F-FDG uptake with superimposed hypermetabolic nodule, whose location corresponds to the original tumor nodule, indicates local recurrence, whereas superimposed focal uptake at a noncorresponding site more likely indicates heterogeneous inflammation around the ablated site.

We also explored rim ratio as a potential parameter for predicting the likelihood of recurrence. Conceptually, higher ratios indicate the presence of larger ablation margins, a known prerequisite for local cure. The rim appearance is caused by ^{18}F-FDG uptake in peripheral inflammatory tissue, and when the margins greatly exceed the boundaries of the original tumor, complete ablation is more probable. The fact that we found a trend toward better recurrence-free survival with higher rim ratios may have been due to the relatively small sample size.

Prior studies suggested that local tumor regrowth was likely when the reduction in SUV from baseline to follow-up study at 2 mo after RFA was less than 60% (*31*). Our data did not show the same trend, but it seems reasonable to assume that minor reductions in SUV between the pre- and postablation scans (or a complete lack thereof) indicate incomplete ablation of the lesion. In our study, the postablation SUV, by itself, was a better predictor of recurrence-free survival, in particular when persisting or increasing during follow-up. Such a pattern is suggestive of regrowth of viable tumor rather than chronic post-RFA inflammation.

As for other indications, imaging with combined ^{18}F-FDG PET/CT offers many advantages over diagnostic CT alone in the pre- and post-RFA assessment of malignant lung lesions. The addition of metabolic information can increase the accuracy of recurrence detection (*31–33*) and allow earlier diagnosis (*31*). In addition, unexpected disease foci may be detected, which may alter management (*34*). PET findings suggestive of local recurrence may precede similar findings on CT, in many cases by 6 mo or more in our patient population. This time interval may be clinically important because smaller tumors would be more amenable to retreatment with RFA or other intervention. A significant lead-time over nonmetabolic imaging alone has been found by other groups (*31*). In some of our cases, the CT showed only nonspecific postablation changes, but biopsies were prompted by abnormal PET findings, proving the presence of disease. A general shortcoming of follow-up with CT alone is the existence of the postablation mass that consists of the original lesion and surrounding normal lung (*28*). Response criteria (such as Response Evaluation Criteria in Solid Tumors) fail in this situation because they rely solely on size (*35*) in a situation in which the postablation mass is almost always larger than the original lesion (if there has been adequate ablation). Some groups have used an arbitrary time interval of 6 mo after ablation, after which any size increase is considered indicative of regrowth (*28*). However, this approach neglects lesions that may regrow within the boundaries of the postablation mass, and it may result in an indeterminate evaluation in the case of a stable lesion on follow-up. Moreover, reliable assessment of post-

RFA findings at 6 mo may be too late because the opportunity for successful retreatment declines with time. Contrast enhancement has also been used as a parameter to evaluate for residual or recurrent tumor after ablation, but lack of contrast enhancement does not necessarily exclude the presence of viable tumor (*25*). Metabolic imaging can enhance evaluation of ablated lesions and obviate sole reliance on parameters such as size and contrast enhancement. In fact, ^{18}F-FDG PET/CT may be of critical importance after thermal ablation, because unlike in surgical resections, there is no evaluable tissue specimen. If validated in further (prospective) studies, ^{18}F-FDG PET may potentially prove essential for the viability of ablation as a therapeutic modality. Early detection of recurrence after ablation is critical because there is an opportunity to repeat the ablation as salvage for recurrence. Successful repeated ablation is best performed on small recurrences rather than large ones.

Our study had some limitations, including its retrospective nature and the lack of standardized imaging follow-up, possibly leading to selection bias. For example, certain tumor types such as sarcoma or small cell carcinoma may be imaged at more frequent intervals because of their aggressiveness or because of patient symptoms or other clinical factors, resulting in skewing of the observed time to progression. In addition, we had a heterogeneous study population, and only a small number of recurrences were indeed confirmed with tissue diagnosis. Our findings should be confirmed by other groups and in a standardized prospective setting. Nevertheless, this is one of the largest studies investigating the utility of ^{18}F-FDG PET/CT after RFA. Because our present findings are sufficiently promising, we are currently working to make PET/CT an integral part of the pre- and post-RFA assessment for lung lesions.

CONCLUSION

Our analysis confirmed the importance of original tumor size in predicting local recurrence. On postablation PET/CT scans, an unfavorable ^{18}F-FDG uptake pattern at the site of the ablated lesion, high postablation SUV, and progressive increase in ^{18}F-FDG uptake during follow-up predicted local recurrence. These findings may help in selecting patients for RFA and in tailoring patient management, including guidance of biopsies to sites of suspected recurrence and early retreatment. Therefore, ^{18}F-FDG PET/CT should be essential in the pre- and posttreatment assessment of patients undergoing RFA for malignant lung lesions.

REFERENCES

1. American Cancer Society. *Cancer Facts and Figures 2008.* Atlanta, GA: American Cancer Society; 2008. Available at: http://www.cancer.org/acs/groups/content/@nho/documents/document/2008cafffinalsecuredpdf.pdf. Accessed October 26, 2010.
2. Dupuy DE, Zagoria RJ, Akerley W, Mayo-Smith WW, Kavanagh PV, Safran H. Percutaneous radiofrequency ablation of malignancies in the lung. *AJR.* 2000;174:57–59.
3. Zhu JC, Yan TD, Morris DL. A systematic review of radiofrequency ablation for lung tumors. *Ann Surg Oncol.* 2008;15:1765–1774.
4. Pua BB, Solomon SB. Radiofrequency ablation of primary and metastatic lung cancers. *Semin Ultrasound CT MR.* 2009;30:113–124.
5. Pennathur A, Abbas G, Schuchert M, Landreneau RJ, Luketich JD. Radiofrequency ablation for the treatment of lung neoplasm. *Expert Rev Med Devices.* 2008;5:613–621.
6. Steinke K, Sewell PE, Dupuy D, et al. Pulmonary radiofrequency ablation: an international study survey. *Anticancer Res.* 2004;24:339–343.
7. Gillams AR, Lees WR. Radiofrequency ablation of lung metastases: factors influencing success. *Eur Radiol.* 2008;18:672–677.
8. Yamagami T, Kato T, Hirota T, et al. Risk factors for occurrence of local tumor progression after percutaneous radiofrequency ablation for lung neoplasms. *Diagn Interv Radiol.* 2007;13:199–203.
9. Pieterman RM, van Putten JW, Meuzelaar JJ, et al. Preoperative staging of non-small-cell lung cancer with positron-emission tomography. *N Engl J Med.* 2000;343:254–261.
10. Lardinois D, Weder W, Hany TF, et al. Staging of non-small-cell lung cancer with integrated positron-emission tomography and computed tomography. *N Engl J Med.* 2003;348:2500–2507.
11. Shim SS, Lee KS, Kim BT, et al. Non-small cell lung cancer: prospective comparison of integrated FDG PET/CT and CT alone for preoperative staging. *Radiology.* 2005;236:1011–1019.
12. Kalff V, Hicks RJ, MacManus MP, et al. Clinical impact of ^{18}F fluorodeoxyglucose positron emission tomography in patients with non-small-cell lung cancer: a prospective study. *J Clin Oncol.* 2001;19:111–118.
13. Gould MK, Kuschner WG, Rydzak CE, et al. Test performance of positron emission tomography and computed tomography for mediastinal staging in patients with non-small-cell lung cancer: a meta-analysis. *Ann Intern Med.* 2003;139:879–892.
14. Hicks RJ, Kalff V, MacManus MP, et al. ^{18}F-FDG PET provides high-impact and powerful prognostic stratification in staging newly diagnosed non-small cell lung cancer. *J Nucl Med.* 2001;42:1596–1604.
15. Dizendorf EV, Baumert BG, von Schulthess GK, Lutolf UM, Steinert HC. Impact of whole-body ^{18}F-FDG PET on staging and managing patients for radiation therapy. *J Nucl Med.* 2003;44:24–29.
16. Feng M, Kong FM, Gross M, Fernando S, Hayman JA, Ten Haken RK. Using fluorodeoxyglucose positron emission tomography to assess tumor volume during radiotherapy for non-small-cell lung cancer and its potential impact on adaptive dose escalation and normal tissue sparing. *Int J Radiat Oncol Biol Phys.* 2009;73:1228–1234.
17. Hicks RJ, Mac Manus MP, Matthews JP, et al. Early FDG-PET imaging after radical radiotherapy for non-small-cell lung cancer: inflammatory changes in normal tissues correlate with tumor response and do not confound therapeutic response evaluation. *Int J Radiat Oncol Biol Phys.* 2004;60:412–418.
18. Dooms C, Verbeken E, Stroobants S, Nackaerts K, De Leyn P, Vansteenkiste J. Prognostic stratification of stage IIIA-N2 non-small-cell lung cancer after induction chemotherapy: a model based on the combination of morphometric-pathologic response in mediastinal nodes and primary tumor response on serial 18-fluoro-2-deoxy-glucose positron emission tomography. *J Clin Oncol.* 2008; 26:1128–1134.
19. Sunaga N, Oriuchi N, Kaira K, et al. Usefulness of FDG-PET for early prediction of the response to gefitinib in non-small cell lung cancer. *Lung Cancer.* 2008;59:203–210.
20. Erdi YE, Nehmeh SA, Mulnix T, Humm JL, Watson CC. PET performance measurements for an LSO-based combined PET/CT scanner using the National Electrical Manufacturers Association NU 2-2001 standard. *J Nucl Med.* 2004;45:813–821.
21. Mawlawi O, Podoloff DA, Kohlmyer S, et al. Performance characteristics of a newly developed PET/CT scanner using NEMA standards in 2D and 3D modes. *J Nucl Med.* 2004;45:1734–1742.
22. Bettinardi V, Danna M, Savi A, et al. Performance evaluation of the new whole-body PET/CT scanner: Discovery ST. *Eur J Nucl Med Mol Imaging.* 2004;31: 867–881.
23. Teras M, Tolvanen T, Johansson JJ, Williams JJ, Knuuti J. Performance of the new generation of whole-body PET/CT scanners: Discovery STE and Discovery VCT. *Eur J Nucl Med Mol Imaging.* 2007;34:1683–1692.
24. Miller R, Siegmund D. Maximally selected chi square statistics. *Biometrics.* 1982;38:1011–1016.
25. Akeboshi M, Yamakado K, Nakatsuka A, et al. Percutaneous radiofrequency ablation of lung neoplasms: initial therapeutic response. *J Vasc Interv Radiol.* 2004;15:463–470.
26. Lee JM, Jin GY, Goldberg SN, et al. Percutaneous radiofrequency ablation for inoperable non-small cell lung cancer and metastases: preliminary report. *Radiology.* 2004;230:125–134.
27. Soret M, Bacharach SL, Buvat I. Partial-volume effect in PET tumor imaging. *J Nucl Med.* 2007;48:932–945.

28. Ambrogi MC, Lucchi M, Dini P, et al. Percutaneous radiofrequency ablation of lung tumours: results in the mid-term. *Eur J Cardiothorac Surg.* 2006;30: 177–183.
29. Thanos L, Mylona S, Pomoni M, et al. Percutaneous radiofrequency thermal ablation of primary and metastatic lung tumors. *Eur J Cardiothorac Surg.* 2006;30:797–800.
30. Rose SC. Radiofrequency ablation of pulmonary malignancies. *Semin Respir Crit Care Med.* 2008;29:361–383.
31. Okuma T, Okamura T, Matsuoka T, et al. Fluorine-18-fluorodeoxyglucose positron emission tomography for assessment of patients with unresectable recurrent or metastatic lung cancers after CT-guided radiofrequency ablation: preliminary results. *Ann Nucl Med.* 2006;20:115–121.
32. Paudyal B, Oriuchi N, Paudyal P, et al. Early diagnosis of recurrent hepatocellular carcinoma with ^{18}F-FDG PET after radiofrequency ablation therapy. *Oncol Rep.* 2007;18:1469–1473.
33. Travaini LL, Trifiro G, Ravasi L, et al. Role of [^{18}F]FDG-PET/CT after radiofrequency ablation of liver metastases: preliminary results. *Eur J Nucl Med Mol Imaging.* 2008;35:1316–1322.
34. Fletcher JW, Djulbegovic B, Soares HP, et al. Recommendations on the use of ^{18}F-FDG PET in oncology. *J Nucl Med.* 2008;49:480–508.
35. Padhani AR, Ollivier L. The RECIST (Response Evaluation Criteria in Solid Tumors) criteria: implications for diagnostic radiologists. *Br J Radiol.* 2001;74: 983–986.